

# Particles and scalar waves in noncommutative charged black hole spacetime

Piyali Bhar,<sup>1,\*</sup> Farook Rahaman,<sup>1,†</sup> Ritabrata Biswas,<sup>2,‡</sup> and U. F. Mondal<sup>3,§</sup>

<sup>1</sup> *Department of Mathematics, Jadavpur University, Kolkata 700 032, West Bengal, India*

<sup>2</sup> *Department of Mathematics, Krishnanagar Women's College,*

*Arobinda Sarani, Krishnanagar, Nadia - 741101, West Bengal, India*

<sup>3</sup> *Department of Mathematics, Behala College, Parnasree, Kolkata 700060, India*

(Dated: June 12, 2015)

In this paper we have discussed geodesics and the motion of test particle in the gravitational field of noncommutative charged black hole spacetime. The motion of massive and massless particle have been discussed separately. A comparative study of noncommutative charged black hole and usual Reissner-Nordström black hole has been done. The study of effective potential has also been included. Finally, we have examined the scattering of scalar waves in noncommutative charged black hole spacetime.

PACS numbers:

## I. INTRODUCTION

Noncommutative geometry (NCG) is concerned with a geometric approach to noncommutative algebras, and with the construction of spaces that are locally presented by noncommutative algebras of functions. Use of such a geometry in cosmological purpose came into existence after the works of Chamseddine, [1, 2]. A general D-Dimensional static spherically symmetric solutions of the specific vector model coupled to Einstein gravity was proposed by [3]. Impact of non commutative geometry on different black holes have been studied by different authors [4]. Surprisingly, it was shown that thermodynamic behavior of the noncommutative Schwarzschild black hole is analogous to that of the Reissner-Nordstrom ( RN ) black hole in the near extremal limit [5]. Alavi worked on a radiating RN black hole in non commutative geometry and establish the facts : the existence of a minimal non-zero mass to which the black hole can shrink; a finite maximum temperature that the black hole can reach before cooling down to absolute zero; compared to the neutral black holes the effect of charge is to increase the minimal non-zero mass and lower the maximum temperature; the absence of any curvature singularity [6]. Three Dimensional Charged Black Hole Inspired by Noncommutative Geometry was studied in [7]. Charged non rotating black holes are been studied in [8]. In [9] by considering particles as smeared objects, Larranaga investigate the effects of space noncommutativity on the geodesic structure in Schwarzschild-AdS spacetime. Considering the effects of noncommutativity in the orbits of particles in Schwarzschild-AdS spacetime it is found that there do exist some For radial time-like geodesics, there are some bounded trajectories. For non-radial time-like geodesics, elliptical orbits are allowed as well as circular orbits.

The usual semiclassical laws of physics break down at plank scale and at this circumstances noncommutativity comes into consideration. The noncommutativity of the spacetime can be encoded by the commutator  $[x^\mu, x^\nu] = i\theta^{\mu\nu}$  where  $\theta^{\mu\nu}$  is the anti-symmetric metric. In literature [10][11] it has been shown that noncommutativity replaces the point-like structure to a smeared objects. The usual definition of mass density function of the commutative space namely Dirac delta function is not so far valid in noncommutative spacetime. In noncommutative space the Dirac delta function is replaced by the gaussian distribution function of the form [12]

$$\rho_\theta = \frac{M}{(4\pi\theta)^{\frac{3}{2}}} e^{-\frac{r^2}{4\theta}} \quad (1)$$

where  $\theta$  is the noncommutative parameter and is of dimension  $length^2$ .

Several authors have described different astrophysical phenomena in noncommutative spacetime. Regular black hole in 3D noncommutative spacetime is analyzed by Myung et al [13]. Baberjee et al [14] have studied noncommutative Schwarzschild Black hole and area law. Three dimensional charged black hole inspired by noncommutative

---

\*Electronic address: piyalibhar90@gmail.com

†Electronic address: rahaman@iucaa.ernet.in

‡Electronic address: biswas.ritabrata@gmail.com

§Electronic address: umarfarooquemondal@ymail.com

geometry has been discussed in [15]. Rahaman et al [16] studied BTZ black hole inspired by noncommutative geometry. Galactic rotation curve in noncommutative geometry background has been analyzed in [17]. Kuhfittig[18] found that a special class of thin shell wormhole that are unstable in classical general relativity but they in a small region in noncommutative spacetime. Higher dimensional wormhole in noncommutative geometry has been discussed in [19]. In that paper authors have shown that the wormhole exists only in four and five dimensional spacetime. Inspired by some of the earlier works [12] [20] [21], in this paper, we will consider noncommutative charged black hole [22]. The underlying fluid is anisotropic in nature but in the limit  $r \gg \sqrt{\theta}$  and  $r \ll \sqrt{\theta}$  it becomes commutative. We shall compare Geodesic study of this black hole with the usual Reissner-Nordström black hole. Next, we will discuss about the motion of a test particle in noncommutative charged black hole spacetime. Finally, we examine the scattering of scalar waves in noncommutative charged black hole spacetime.

The plan of the present paper as follows: In section II we have discussed about noncommutative charged black hole. In section III geodesic study has been done (massless and massive particle have been discussed separately). In section IV, we have discussed about effective potential and in section V motion of test particle have been studied. In section VI, we have examined the scattering of scalar waves in noncommutative charged black hole spacetime and lastly some concluding remarks have been included.

## II. NONCOMMUTATIVE CHARGED BLACK HOLE

The metric of a noncommutative charged black hole is described by the metric given by [22],

$$ds^2 = - \left( 1 - \frac{2M_\theta}{r} + \frac{Q_\theta^2}{r^2} \right) dt^2 + \left( 1 - \frac{2M_\theta}{r} + \frac{Q_\theta^2}{r^2} \right)^{-1} dr^2 + r^2 d\Omega^2 \quad (2)$$

where

$$M_\theta(r) = \frac{2M}{\sqrt{\pi}} \gamma \left( \frac{3}{2}, \frac{r^2}{4\theta} \right)$$

$$Q_\theta(r) = \frac{Q}{\sqrt{\pi}} \sqrt{\gamma^2 \left( \frac{1}{2}, \frac{r^2}{4\theta} \right) - \frac{r}{\sqrt{2\theta}} \gamma \left( \frac{1}{2}, \frac{r^2}{2\theta} \right)}$$

$$\gamma \left( \frac{a}{b}, x \right) = \int_0^x u^{\frac{a}{b}-1} e^{-u} du \quad (3)$$

The horizon radius is  $r_h$  where  $f(r_h) = 0$  i.e. where  $f(r)$  cuts the  $r$  axis (see fig.1).

Here,

$$f(r) = 1 - \frac{4M}{r\sqrt{\pi}} \gamma \left( \frac{3}{2}, \frac{r^2}{4\theta} \right) + \frac{Q^2}{r^2\pi} \left[ \gamma^2 \left( \frac{1}{2}, \frac{r^2}{4\theta} \right) - \frac{r}{\sqrt{2\theta}} \gamma \left( \frac{1}{2}, \frac{r^2}{2\theta} \right) \right] \quad (4)$$

where  $M$  is the mass and  $Q$  is the charge of the black hole. It is noted that for large  $r$ , Reissner-Nordström black hole will be obtained.

The horizon radius ( $r_h$ ) can be found where  $f(r_h) = 0$  in other words, where  $f(r)$  cuts  $r$  axis (see fig-1). We observe that for specific values of the parameters, say,  $M=2$ ,  $Q=1$  and  $\theta = 0.1$ , we get two radii of horizons where outer horizon exists at  $r_h = 0.9267$ .

## III. THE GEODESICS

Without loss of generality, let us consider the geodesic motion in the plane  $\vartheta = \frac{\pi}{2}$ . From the geodesics equation

$$\frac{dx^\mu}{d\tau^2} + \Gamma_{\nu\lambda}^\mu \frac{dx^\nu}{d\tau} \frac{dx^\lambda}{d\tau} = 0, \quad (5)$$

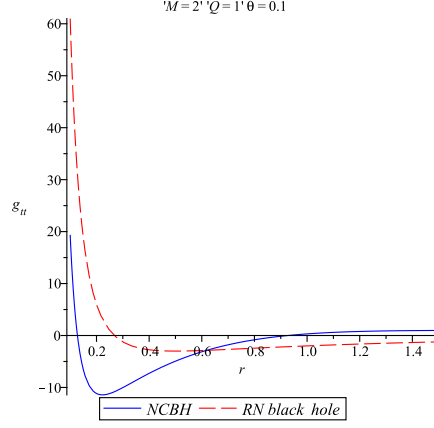


FIG. 1: Two horizons exist for Noncommutative charged black hole.

one can obtain

$$\frac{1}{f(r)} \left( \frac{dr}{d\tau} \right)^2 = \frac{E^2}{f(r)} - \frac{J^2}{r^2} - L \quad (6)$$

$$r^2 \left( \frac{d\phi}{d\tau} \right) = J \quad (7)$$

and

$$\frac{dt}{d\tau} = \frac{E}{f(r)} \quad (8)$$

where  $f(r)$  is given in (4) and the constants  $E$  and  $J$  are energy per unit mass and angular momentum respectively about an axis invariant to the plane  $\theta = \frac{\pi}{2}$ . Here  $\tau$  is the affine parameter and  $L$  is the Lagrangian having value 0 and 1 respectively for massless and massive particle.

Now for radial geodesic ( $J = 0$ ). Then from equation (6) we get,

$$\left( \frac{dr}{d\tau} \right)^2 = E^2 - Lf(r) \quad (9)$$

Using the equations (8) and (9), we get,

$$\left( \frac{dr}{dt} \right)^2 = \{f(r)\}^2 \left[ 1 - \frac{L}{E^2} f(r) \right] \quad (10)$$

#### A. For photon Like Particle (L=0)

For photon like particle we have,

$$\left( \frac{dr}{dt} \right)^2 = \left\{ 1 - \frac{4M}{r\sqrt{\pi}} \gamma \left( \frac{3}{2}, \frac{r^2}{4\theta} \right) + \frac{Q^2}{r^2\pi} \left[ \gamma^2 \left( \frac{1}{2}, \frac{r^2}{4\theta} \right) - \frac{r}{\sqrt{2\theta}} \gamma \left( \frac{1}{2}, \frac{r^2}{2\theta} \right) \right] \right\}^2, \quad (11)$$

which gives,

$$\pm t = \int_{r_h}^{r^*} \frac{dr}{1 - \frac{4M}{r\sqrt{\pi}} \gamma \left( \frac{3}{2}, \frac{r^2}{4\theta} \right) + \frac{Q^2}{r^2\pi} \left[ \gamma^2 \left( \frac{1}{2}, \frac{r^2}{4\theta} \right) - \frac{r}{\sqrt{2\theta}} \gamma \left( \frac{1}{2}, \frac{r^2}{2\theta} \right) \right]} \quad (12)$$

TABLE I: Values of  $t$  for different  $r$ .  $r_h = 0.9267$ ,  $\theta = 0.1, M = 2, Q = 1$ 

$r$	$t$
2	1.2014
2.5	1.7014
3	2.2014
3.5	2.7014
4	3.2014
4.5	3.7014

TABLE II: Values of  $t$  for different  $r$ .  $r_h = 0.9267$ ,  $\theta = 0.1, M = 2, Q = 1, E = 1.5$ 

$r$	$t$
2	1.2340
2.5	1.7504
3	2.2668
3.5	2.7832
4.5	3.8160
5	4.3324

The above integration can not be performed analytically but by the help of numerical integration one can obtain the values of  $t$  for different values of  $r$  which has shown in TABLE-1.

The relation between the distance( $r$ ) and time ( $t$ ) has been plotted in **fig.2**.

From equation (9) we get,

$$\left(\frac{dr}{d\tau}\right)^2 = E^2 \quad (13)$$

which gives,

$$r = \pm E\tau \quad (14)$$

The relation between the distance  $r$  and proper time ( $\tau$ ) has been plotted in **fig.2**

### B. Massive Particle Motion(L=1)

From equations (6) and (8), we obtain

$$\left(\frac{dr}{dt}\right)^2 = \left(\frac{f(r)}{E^2}\right)^2 (E^2 - f(r)) \quad (15)$$

which implies,

$$\pm t = \int_{r_h}^{r^*} \frac{E dr}{\left\{1 - \frac{4M}{r\sqrt{\pi}}\gamma\left(\frac{3}{2}, \frac{r^2}{4\theta}\right) + \frac{Q^2}{r^2\pi} \left[\gamma^2\left(\frac{1}{2}, \frac{r^2}{4\theta}\right) - \frac{r}{\sqrt{2\theta}}\gamma\left(\frac{1}{2}, \frac{r^2}{2\theta}\right)\right]\right\} \sqrt{E^2 - 1 + \frac{4M}{r\sqrt{\pi}}\gamma\left(\frac{3}{2}, \frac{r^2}{4\theta}\right) - \frac{Q^2}{r^2\pi} \left[\gamma^2\left(\frac{1}{2}, \frac{r^2}{4\theta}\right) - \frac{r}{\sqrt{2\theta}}\gamma\left(\frac{1}{2}, \frac{r^2}{2\theta}\right)\right]}} \quad (16)$$

As before, the above integration can not be obtained analytically, so we obtain the numerical values of  $t$  for different values of  $r$  which has shown in TABLE-2

The relation between the distance( $r$ ) and time ( $t$ ) has been plotted in **fig.3**

From equation (9) we get,

$$\left(\frac{dr}{d\tau}\right)^2 = E^2 - f(r) \quad (17)$$

TABLE III: Values of  $t$  for different  $r$ .  $r_h = 0.9267$ ,  $\theta = 0.1, M = 2, Q = 1, E = 1.5$ 

$r$	$t$
2	0.9108
2.5	1.3580
3	1.8052
3.5	2.2524
4	2.6996
4.5	3.1468

which gives,

$$\pm \tau = \int_{r_h}^r \frac{dr}{\sqrt{E^2 - 1 + \frac{4M}{r\sqrt{\pi}}\gamma\left(\frac{3}{2}, \frac{r^2}{4\theta}\right) - \frac{Q^2}{r^2\pi}\left[\gamma^2\left(\frac{1}{2}, \frac{r^2}{4\theta}\right) - \frac{r}{\sqrt{2\theta}}\gamma\left(\frac{1}{2}, \frac{r^2}{2\theta}\right)\right]}} \quad (18)$$

Again, the above integration can not be solved analytically, so we obtain the numerical values of  $t$  for different values of  $r$  which has shown in TABLE. 3

The relation between the distance( $r$ ) and proper time ( $\tau$ ) has been plotted in **fig.3**.

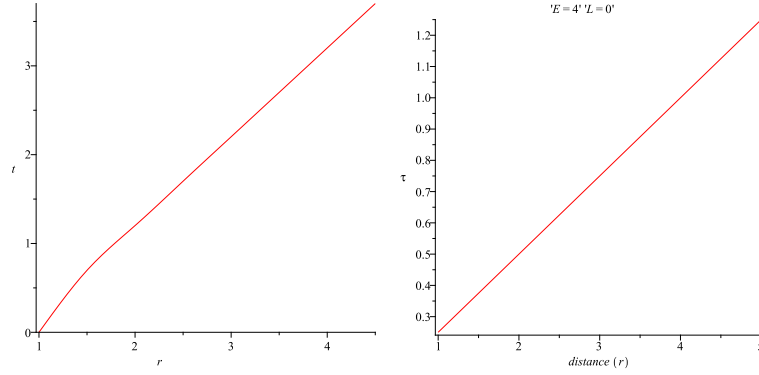


FIG. 2: (Left) Variation of  $t$  has been plotted against  $r$  for massless particle. (Right) Variation of proper time ( $\tau$ ) has been plotted against  $r$  for massless particle.

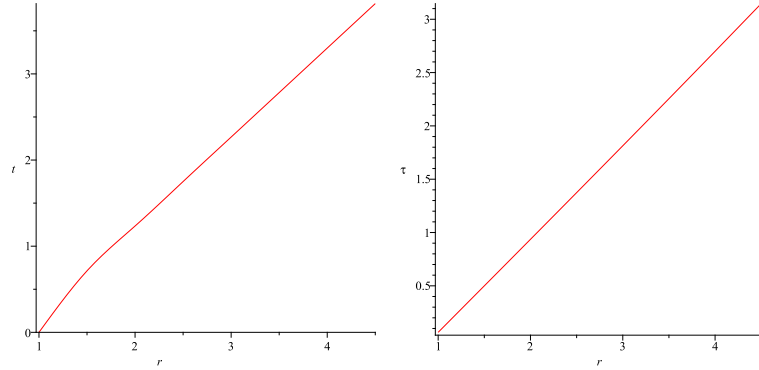


FIG. 3: (Left) Variation of  $t$  has been plotted against  $r$  for massive particle. (Right) Variation of proper time ( $\tau$ ) has been plotted against  $r$  for massive particle.

#### IV. EFFECTIVE POTENTIAL

From equation (6) we get,

$$\frac{1}{2} \left( \frac{dr}{d\tau} \right)^2 = \frac{1}{2} \left[ E^2 - f(r) \left( L + \frac{J^2}{r^2} \right) \right] \quad (19)$$

Now comparing the equation ( ) with the equation  $\frac{\dot{r}^2}{2} + V_{eff} = 0$ , one can get the effective potential as,

$$V_{eff} = -\frac{1}{2} \left[ E^2 - f(r) \left( L + \frac{J^2}{r^2} \right) \right] \quad (20)$$

##### A. For Photonlike Particle (L=0)

Now for radial geodesics  $p = 0$ . In that case  $V_{eff}$  is given by

$$V_{eff} = -\frac{1}{2} E^2$$

Now if  $E = 0$ ,  $V_{eff}$  becomes zero and the particle behaves "like a free" particle. So we will consider the case  $p \neq 0$ . Then  $V_{eff}$  becomes,

$$V_{eff} = -\frac{E^2}{2} + \frac{J^2}{2r^2} \left[ 1 - \frac{4M}{r\sqrt{\pi}} \gamma \left( \frac{3}{2}, \frac{r^2}{4\theta} \right) + \frac{Q^2}{r^2\pi} \left\{ \gamma^2 \left( \frac{1}{2}, \frac{r^2}{4\theta} \right) - \frac{r}{\sqrt{2\theta}} \gamma \left( \frac{1}{2}, \frac{r^2}{2\theta} \right) \right\} \right] \quad (21)$$

As  $r \rightarrow 0$  the effective potential  $V_{eff}$  becomes very large. As  $r \rightarrow \infty$ ,  $V_{eff}$  becomes  $-\frac{E^2}{2}$  and at the horizon  $V_{eff} = -\frac{E^2}{2}$

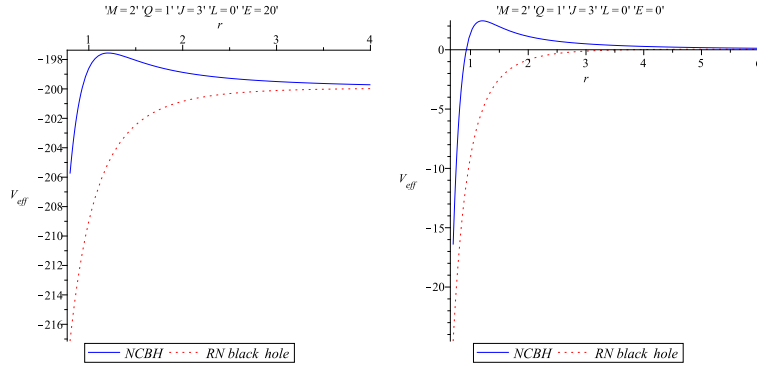


FIG. 4: (Left)  $V_{eff}$  has been plotted against  $r$  for massless particle when  $E \neq 0$ . (Right)  $V_{eff}$  has been plotted against  $r$  for massless particle when  $E = 0$ .

##### B. For Timelike particle (L=1)

For timelike particle effective potential  $V_{eff}$  becomes,

$$V_{eff} = -\frac{E^2}{2} + \frac{1}{2} \left( 1 + \frac{J^2}{r^2} \right) \left[ 1 - \frac{4M}{r\sqrt{\pi}} \gamma \left( \frac{3}{2}, \frac{r^2}{4\theta} \right) + \frac{Q^2}{r^2\pi} \left\{ \gamma^2 \left( \frac{1}{2}, \frac{r^2}{4\theta} \right) - \frac{r}{\sqrt{2\theta}} \gamma \left( \frac{1}{2}, \frac{r^2}{2\theta} \right) \right\} \right] \quad (22)$$

The effective potential becomes very large as  $r \rightarrow 0$  and  $\frac{1-E^2}{2}$  as  $r \rightarrow \infty$ .

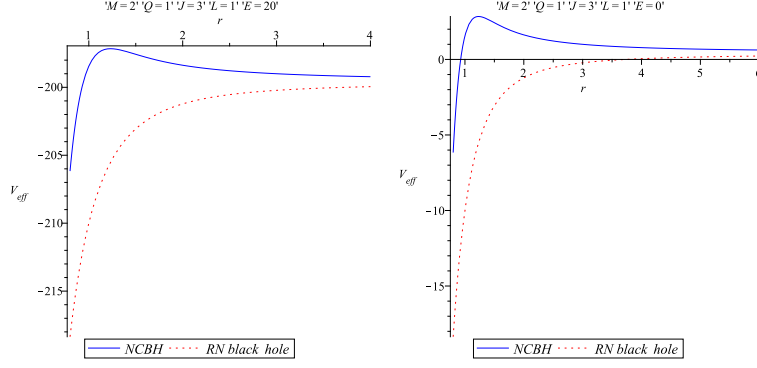


FIG. 5: (Left)  $V_{eff}$  has been plotted against  $r$  for massive particle when  $E \neq 0$ . (Right)  $V_{eff}$  has been plotted against  $r$  for massive particle when  $E = 0$ .

We note that for the above choices of the parameters, say,  $M=2$ ,  $Q=1$  and  $\theta = 0.1$ , the potential has no extremals for photon like particle, however, for massive particle, the potential has two extremals. At  $r = r_h$ ,

$$V_{eff} = -\frac{E^2}{2},$$

for massless and massive particles. Also it is found that potential has a local maximum near the horizon. We should mention that for RN black hole, potential has one extremal but no local maximum point.

## V. TEST PARTICLE MOTION AROUND NONCOMMUTATIVE CHARGED BLACK HOLE

In this section we will consider the motion of test particle around non commutative noncommutative charged black hole using Hamilton-Jacobi [ H-J ] approach. We assume that a test particle of mass  $m$  and charge  $e$  moving in the gravitational field of the noncommutative charged black hole. The Hamilton-Jacobi [ H-J ] equation for the test particle is given by

$$g^{ik} \left( \frac{\partial S}{\partial x^i} + eA_i \right) \left( \frac{\partial S}{\partial x^k} + eA_k \right) + m^2 = 0, \quad (23)$$

where  $A_i$  is the gauge potential and  $g_{ik}$  represents the classical background field and  $S$  is the standard Hamilton's characteristic function.

One can write the explicit form of H-J equation for the metric (2) as [23]

$$-\frac{1}{f} \left( \frac{\partial S}{\partial t} + \frac{eQ}{r} \right)^2 + f \left( \frac{\partial S}{\partial r} \right)^2 + \frac{1}{r^2} \left( \frac{\partial S}{\partial \vartheta} \right)^2 + \frac{1}{r^2 \sin^2 \vartheta} \left( \frac{\partial S}{\partial \phi} \right)^2 + m^2 = 0 \quad (24)$$

This partial equation can be solved using the separation of variables method. We choose the  $H - J$  function  $S$  in separable form as

$$S(t, r, \theta, \phi) = -E.t + S_1(r) + S_2(\vartheta) + J.\phi,$$

where  $E$  is the energy of the particle and  $J$  is the angular momentum of the particle.

The radial velocity of the particle takes the form

$$\frac{dr}{dt} = f^2 \left( E - \frac{eQ}{r^2} \right)^{-1} \sqrt{\frac{1}{f^2} \left( E - \frac{eQ}{r} \right)^2 - \frac{m^2}{f} - \frac{p^2}{fr^2}} \quad (25)$$

The turning points of the trajectory can be obtained through the equation  $\left( \frac{dr}{dt} \right) = 0$  and we get

$$\left(E - \frac{eQ}{r}\right)^2 - m^2 f - \frac{p^2}{r^2} f = 0.$$

This equation implies

$$E = \frac{eQ}{r} + \sqrt{f} \left(m^2 + \frac{p^2}{r^2}\right)^{1/2}$$

Therefore, the potential curve takes the form as

$$V(r) \equiv \frac{E}{m} = \frac{eQ}{mr} + \sqrt{f} \left(1 + \frac{p^2}{m^2 r^2}\right)^{1/2}$$

i.e.

$$V(r) = \frac{eQ}{mr} + \sqrt{\left(1 + \frac{p^2}{m^2 r^2}\right)} \sqrt{1 - \frac{4M}{r\sqrt{\pi}} \gamma\left(\frac{3}{2}, \frac{r^2}{4\theta}\right) + \frac{Q^2}{r^2 \pi} \left[\gamma^2\left(\frac{1}{2}, \frac{r^2}{4\theta}\right) - \frac{r}{\sqrt{2\theta}} \gamma\left(\frac{1}{2}, \frac{r^2}{2\theta}\right)\right]} \quad (26)$$

For a stationary situation,  $E$  i.e.  $V(r)$  should have an extremal value. Hence for the extremal case

$$\frac{dV}{dr} = 0, \quad (27)$$

which gives

$$\frac{eQ}{mr^2} \sqrt{f} \left(1 + \frac{p^2}{m^2 r^2}\right)^{1/2} = \frac{1}{2} \left(1 + \frac{p^2}{m^2 r^2}\right) f'(r) - f \frac{p^2}{m^2 r^3} \quad (28)$$

#### A. Test particle in Static Equilibrium ( $p=0$ )

Note that momentum  $p$  should vanish in static equilibrium. Therefore, we find the value of  $r$  for which potential is extremal is given by

$$H(r) \equiv \frac{eQ}{mr^2} \sqrt{f} - \frac{1}{2} f' = 0 \quad (29)$$

where  $f(r)$  is given in equation (3).

Equation (28) has at least one real root where  $H(r)$  cuts the  $r$  axis. (see *fig - 6*). Hence it is possible to have bound orbit for the test particle. In other words charged particle can be trapped by the noncommutative charged black hole in static equilibrium.

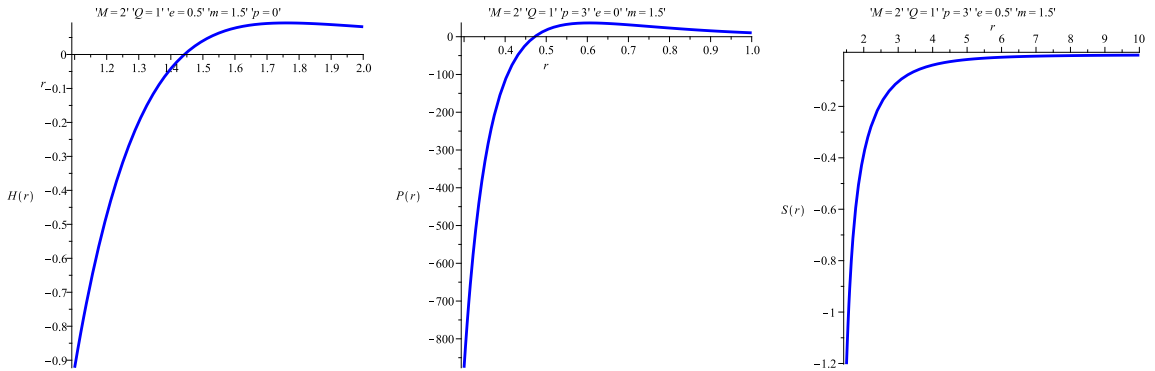


FIG. 6: (Left) Real root exists . (Middle) Real root exists . (Right) Real root does not exist.



## B. Test particle in Non-Static Equilibrium

### 1. Uncharged test particle ( $e = 0$ )

Now the expression (27) simplifies to

$$P(r) \equiv \frac{1}{2} \left( 1 + \frac{p^2}{r^2 m^2} \right) f' + f \frac{p^2}{m^2 r^3} = 0 \quad (30)$$

where  $f(r)$  is given in equation (3).

Equation (28) has at least one real root where  $P(r)$  cuts the  $r$  axis (see *fig-6*). Hence it is possible to have bound orbit for the test particle. In other words, non-charged particle can be trapped by the noncommutative charged black hole in non-static equilibrium.

### 2. Test particle with charge ( $e \neq 0$ )

From eqn.(27), we have

$$S(r) \equiv \frac{eQ}{mr^2} \sqrt{f} \left( 1 + \frac{p^2}{m^2 r^2} \right)^{1/2} - \frac{1}{2} \left( 1 + \frac{p^2}{m^2 r^2} \right) f'(r) + f \frac{p^2}{m^2 r^3} \quad (31)$$

where  $f(r)$  is given in equation (3).

Equation (29) has no real root since  $S(r)$  does not cut the  $r$  axis (see *fig-6*). Hence it is not possible to have bound orbit for the test particle. Hence, charged particle can not be trapped by the noncommutative charged black hole in non-static equilibrium. The possible reason for this behavior is that noncommutative charged black hole exerts repulsive force on charged particle.

## VI. SCATTERING OF SCALAR WAVES IN NONCOMMUTATIVE CHARGED BLACK HOLE GEOMETRY

The wave equation for minimally coupled massless test scalar  $\Phi$  in noncommutative charged black hole background is given by

$$\square \Phi = \frac{1}{\sqrt{-g}} \partial_\mu [\sqrt{-g} g^{\mu\nu} \partial_\nu \Phi] = 0. \quad (32)$$

Since the noncommutative charged black hole spacetime is spherically symmetric, the scalar field can be separated by the variables

$$\Phi_{lm} = Y_{lm}(\theta, \phi) \frac{U_l(r, t)}{r}. \quad (33)$$

where  $Y_{lm}(\theta, \phi)$  is the spherical harmonics and  $l$  is the quantum angular momentum. Using the separable form (35) in (34), we find

$$\left[ \frac{1}{\sin \theta} \frac{\partial}{\partial \theta} \sin \theta \frac{\partial}{\partial \theta} + \frac{1}{\sin^2 \theta} \frac{\partial^2}{\partial \phi^2} \right] Y_{lm} = l(l+1) Y_{lm}, \quad (34)$$

$$\ddot{U}_l + \frac{\partial^2 U_l}{\partial r^{*2}} = V_l U_l. \quad (35)$$

where the potential  $V_l$  is given by

$$V_l = \left[ 1 - \frac{4M}{r\sqrt{\pi}} \gamma \left( \frac{3}{2}, \frac{r^2}{4\theta} \right) + \frac{Q^2}{r^2 \pi} \left\{ \gamma^2 \left( \frac{1}{2}, \frac{r^2}{4\theta} \right) - \frac{r}{\sqrt{2\theta}} \gamma \left( \frac{1}{2}, \frac{r^2}{2\theta} \right) \right\} \right] \times$$

TABLE IV: Values of  $r^*$  for different  $r$ . ( $r_h = 0.9267$ ,  $\theta = 0.1$ ,  $M = 2$ ,  $Q = 1$ )

$r$	$t$
4	3.8794
4.5	4.3794
5	4.8794
5.5	5.3794
6	5.8794
6.5	6.3794
7	6.8794

$$\left[ \frac{l(l+1)}{r^2} + \frac{1}{r} \left\{ \frac{4M}{r^2 \sqrt{\pi}} \gamma \left( \frac{3}{2}, \frac{r^2}{4\theta} \right) + \frac{Mr}{\theta^{\frac{3}{2}} \sqrt{\pi}} e^{-\frac{r^2}{4\theta}} \right\} + \frac{Q^2}{r^3 \pi} \left\{ -\frac{2}{r} \gamma^2 \left( \frac{1}{2}, \frac{r^2}{4\theta} \right) + \frac{1}{\sqrt{2\theta}} \gamma \left( \frac{1}{2}, \frac{r^2}{2\theta} \right) - 2\sqrt{\frac{\pi}{\theta}} e^{-\frac{r^2}{4\theta}} \operatorname{erfc} \left( \frac{r}{2\sqrt{\theta}} \right) \right\} \right]$$

Here, we have used tortoise coordinate transformation  $r^*$  as

$$\frac{\partial}{\partial r^*} = \left[ 1 - \frac{4M}{r\sqrt{\pi}} \gamma \left( \frac{3}{2}, \frac{r^2}{4\theta} \right) + \frac{Q^2}{r^2 \pi} \left\{ \gamma^2 \left( \frac{1}{2}, \frac{r^2}{4\theta} \right) - \frac{r}{\sqrt{2\theta}} \gamma \left( \frac{1}{2}, \frac{r^2}{2\theta} \right) \right\} \right] \frac{\partial}{\partial r}. \quad (36)$$

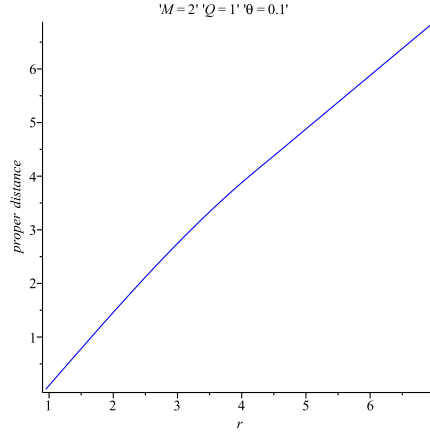
[ dot represents the differentiation with respect to  $t$  ]

The proper distance  $r^*$  can be expressed as

$$r^* = \int_{r_h}^r \frac{dx}{\left[ 1 - \frac{4M}{x\sqrt{\pi}} \gamma \left( \frac{3}{2}, \frac{x^2}{4\theta} \right) + \frac{Q^2}{x^2 \pi} \left\{ \gamma^2 \left( \frac{1}{2}, \frac{x^2}{4\theta} \right) - \frac{x}{\sqrt{2\theta}} \gamma \left( \frac{1}{2}, \frac{x^2}{2\theta} \right) \right\} \right]}. \quad (37)$$

Note that this integration cannot be solved analytically form, therefore, we find the numerical values of the proper distance  $r^*$  for given values of radial distance  $r$  from the horizon radius  $r_h$  ( see Table 4 ).

The variation of proper distance ( $r^*$ ) with radial distance  $r$  is depicted in Fig. 7.

FIG. 7: A plot of the proper distance ( $r^*$ ) versus  $r$ .

For time dependent harmonic wave, we can write

$$U_l(r, t) = \hat{U}_l(r, \omega) e^{-i\omega t} \quad (38)$$

Using (38) in (35) we get the Schrödinger equation

$$\left[ \frac{d^2}{dr^{*2}} + \omega^2 - V_l(r) \right] \hat{U}_l(r, \omega) = 0 \quad (39)$$

It is observed that  $V_l$  tends to zero as  $r \rightarrow \infty$ . This implies that the solution has the type of a plane wave  $\hat{U}_{l_0} \sim e^{\pm i\omega r^*}$  asymptotically which is purely outgoing wave. At the horizon,  $V_l \rightarrow 0$  and is purely ingoing wave. This indicates that if a scalar wave is going through the gravitational field of a noncommutative charged black hole, the nature of the solution would be changed from  $e^{\pm i\omega r}$  into  $e^{\pm i\omega r^*}$ . In other words, the potential will be affected by the scattering of scalar waves. The potentials are depicted in figure 8.

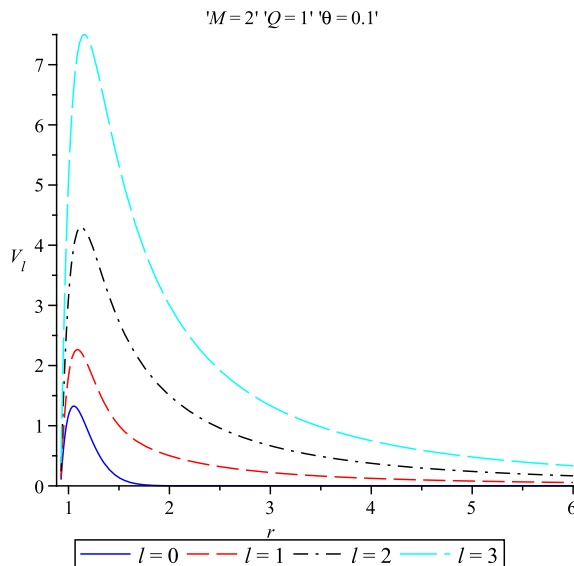


FIG. 8: A plot of the potentials of the scalar wave for  $l=0,1,2,3$ .

## VII. CONCLUSION

Noncommutativity is coming actually from the string theory that is replaced by the usual point-like structure by smeared objects. Therefore, in a natural way the usual definition of Dirac-delta function replaces everywhere with Gaussian distribution of minimal width  $\sqrt{\theta}$ , where  $\theta$  is the non-commutative parameter. In our present article, we have analyzed the behavior of the time like and null geodesics of the non-commutative R-N black hole. The Variation of time ( $t$ ) and the proper time ( $\tau$ ) have been explored graphically by plotting against radial distance ( $r$ ) for both massless and massive particle. Also, the nature of the effective potential has been shown by plotting against  $r$  for massless particle when  $E \neq 0$  as well as  $E = 0$ . In case of photon like and time like particle for  $E = 0$  the root of the effective potential coincides with the root of the non-commutative RN black hole. From our analysis it is shown that for both case of charged particle in static equilibrium and uncharged test particle in non-Static equilibrium, particles can be trapped by the noncommutative charged black hole, where as in case of uncharged particle in non static equilibrium it is not possible to have bound orbit for the test particle. So uncharged particle can not be trapped by the noncommutative charged black hole in the case of non-static equilibrium. The possible reason for this behavior is that noncommutative charged black hole exerts repulsive force on uncharged particle. We have also compared the behavior of the time-like and null geodesics between Non-commutative R-N Black Hole and R-N black hole. It is also shown that for  $r \rightarrow \infty$  the non-commutative R-N Black hole comes back to the R-N black hole. Finally we studied the scattering problem of the scalar wave in noncommutative R-N black hole geometry. It is seen that the potential will be affected by the scattering of scalar waves. The characteristic of the potential is shown graphically. For  $Q = 0$  our results coincide with non charged case [24].

## ACKNOWLEDGMENTS

FR and RB would like to thank Inter-University Centre for Astronomy and Astrophysics (IUCAA), Pune, India for providing research facilities.

- 
- [1] Chamseddine, A. H., Felder, G., Frohlich, J. , *Commun. Math. Phys.* **155** (1993), 205
  - [2] Klimcik, C., Pompos, A., Soucek, V. , *Letters in Math. Phys.* **30** (1994) 259.
  - [3] Klimcik, C., Kolnik, P., Pompos, A. , gr-qc/9405012.
  - [4] Naseri, F. , *Gen.Rel.Grav.* **37** (2005) 2223; Nicolini, P., Smailagic, A., Spallucci, E. , *Phys.Lett. B* **632** (2006) 547; Sadeghi, J., Setare, M.R. :- *Int.J.Theor.Phys.* **46** (2007) 817.
  - [5] Kim, W., Son, E. J., Yoon, M. :- *JHEP* **0804** (2008) 042.
  - [6] Alavi, S.A. , *Acta Phys.Polon.* **B40** (2009) 2679.
  - [7] Larranaga, A., Tejeiro, J. M., *Abraham Zelmanov J.* **4** (2011) 28.
  - [8] Modesto, L., , Nicolini, P. ,*Phys.Rev. D* **82** (2010) 104035.
  - [9] Larranaga, A , *Rom.J.Phys.* **58** (2013) 50.
  - [10] A. Smailagic , E. Spallucci ,*J. Phys.A* **36** ,L467 (2003)
  - [11] T.G.Rizzo, *J.High Energy Phys.* **09**,021 (2006)
  - [12] P.nicoloni ,A.Smailagic and E. Spalluci, *Phys. Lett B* **632**,547 (2006)
  - [13] Yun Soo Myung, Myungseok Yoon, **arXiv:0810.0078v2[gr-qc]**
  - [14] Rabin Banerjee, Bibhas Ranjan Majhi and Sujoy Kumar Modak, **arXiv:0802.2176v2 [hep-th]**
  - [15] Alexis Larrañaga, Juan Mnuel Tejeiro, **arXiv:1004.1608v1 [gr-qc]**
  - [16] Farook Rahaman, P.K.F.Kuhfittig, B.C.Bhui, Mosiur Rahaman, Saibal Ray, U.F.Mondal, *Phys.Rev D***87**, 084014 (2013)
  - [17] F.Rahaman, P.K.F.Kuhfittig, K.Chakraborty, A.A.Usmani and S.Ray, *Gen Relativ.Gravit.* **44**, 905 (2012)
  - [18] P.K.F.Kuhfittig, *Adv.High Energy Phys***2012**, 462493 (2012)
  - [19] F.Rahaman, P.K.F.Kuhfittig, S.Ray and S Islam, *Phys. Rev D* **86**, 106010 (2012)
  - [20] E.Di Grezia, G Esposito, *Int.J.Geom.Meth.Mod.Phys* **08**,657 (2011)
  - [21] M.Chabab et al., **arXiv:1201.2547**
  - [22] S. Ansoldi et al., *Phys. Lett.B* **645** 261 (2007).
  - [23] S. Chakraborty and F. Rahaman, *Pramana* **51** , 689 (1998); Farook Rahaman, *Int.J.Mod.Phys. D* **9**, 627 (2000)
  - [24] F. Rahaman et al, *Particles Motion Around a Non-Commutative Black Hole*, *Int.J.Theor.Phys.* **54**, 1038 (2015).